Switching of Molecular Spin States in Inorganic Complexes by Temperature, Pressure, Magnetic Field and Light: Towards Molecular Devices

Azzedine Bousseksou,*[a] Gábor Molnár,[a] and Galina Matouzenko[b]

Keywords: Spin crossover / Metastability / Hysteresis loop / Pressure / Magnetic field / Dielectric properties / Ising-like model

The spin crossover phenomenon in molecular inorganic compounds is one of the most spectacular examples of bistability phenomena leading to a switching between the high-spin and the low-spin states of the molecule by several means such as temperature, pressure, light and magnetic field (multi-property molecular switching). In the present microreview we report our most important findings, both experimental results and theoretical approaches, and discuss possible technological applications for each switching method as well as the recent synthesis of new spin crossover molecular materials.

1. Introduction

Certain (pseudo)octahedral transition metal complexes are known to display a molecular bistability of the high-spin (HS) and low-spin (LS) electron configurations which can be distinguished by different occupations of the antibonding e_g and the nonbonding t_{2g} d orbitals of the central metal ion.[1,2] The electronic ground state of these spin crossover (SCO) complexes may be reversibly interchanged by an external stimulus such as temperature, pressure, magnetic field or light irradiation. This phenomenon was discovered by Cambi et al. as part of a study of iron(III) dithio-

[a] Laboratoire de Chimie de Coordination, UPR 8241 CNRS, 205 route de Narbonne, 31077 Toulouse, France
E-mail: boussek@lcc-toulouse.fr
[b] Laboratoire de Chimie (UMR CNRS and ENS-Lyon No. 5182), Ecole Normale Supérieure de Lyon, 46, allée d'Italie, 69364 Lyon, France

Azzedine Bousseksou was born in 1964 in Algiers, Algeria, and received his Ph.D. in solid state physics from the University of Paris 6 (Pierre et Marie Curie) in 1992. He was a Research Associate at the University of Paris 6 with the group of François Varret (Physics Research Department) for one year. In 1993 he received a permanent position as a "Chargé de Recherche" at the CNRS. In 1997 he joined the Laser Laboratory and Raman spectroscopy group of Prof. John McGarvey in N. Ireland for 18 months. In 1997, he was promoted to first class of "Chargé de Recherche-CNRS". He presently leads the team "Molecular Physics Properties" at the Laboratoire de Chimie de coordination CNRS Toulouse. His field of research includes molecular bistability and molecular spin-crossover phenomena, experimental and theoretical approaches, thin films, and nanostructures and devices; he published approximately 80 articles, 2 patents, 3 book chapters and organised several workshops, he is a member of the national comity of the CNRS (2000−2004). He was awarded the 2003 prize for the Coordination Chemistry Division of the French Chemical Society.

Gábor Molnár was born in Szolnok (Hungary) in 1973. He received his M.Sc. degree in 1996 from the Eötvös Loránd University (Budapest, Hungary). He prepared his Ph.D. thesis under the supervision of P. Iacconi (University of Nice, France) and J. Borossay (Eötvös University) in the field of thermoluminescent dosimeter materials. He held a postdoctoral position for 8 months at the IMRA-Europe company (Sophia Antipolis, France) and worked on photovoltaic materials. He then joined the group of J. J. McGarvey as a Marie Curie fellow for 12 months at the Queens University of Belfast (U.K.) to develop a new high-pressure Raman spectroscopy setup. In 2002, he became Research Associate ("poste rouge") at the CNRS Laboratoire de Chimie de Coordination (Toulouse, France) where he later received a permanent position with the group of A. Bousseksou. His current research focuses on molecular bistability and molecular spin-crossover phenomena.

Galina Matouzenko obtained her undergraduate degree at Kishinev University (USSR) and her Ph.D. degree from the Institute of Chemistry, Moldavian Academy of Sciences working with Professor A. V. Ablov, one of the leading Soviet coordination chemists. Her thesis focused on the synthesis, magnetic properties and magneto-structural correlations in new exchange-coupled polynuclear complexes of transition metals. After coming to France, in 1992 she joined the Laboratory of Chemistry, UMR (Unité Mixte de Recherche) of the CNRS and Ecole Normale Supérieure de Lyon. Her current interests lie in the field of the design of new mono- and polymeric spin-transition systems.

MICROREVIEWS: This feature introduces the readers to the authors' research through a concise overview of the selected topic. Reference to important work from others in the field is included.

carbamate compounds in the early 1930s.[3] The first Fe^{II} complexes $[Fe(phen)_2(NCS)_2]$ and $[Fe(bipy)_2(NCS)_2]$ (phen = 1,10-phenanthroline, bipy = 2,2-bipyridine) with "unusual magnetic behaviour" were reported only about 30 years later.[4] Their careful reinvestigation by König[5] has shown that they represent the first examples of iron(II) SCO compounds and this marked a starting point for further extensive developments of the field, chiefly in the framework of the European TOSS TMR network coordinated by P. Gütlich.[6] Although the SCO phenomenon may occur for octahedral compounds with d^4-d^7 configurations, it is most commonly observed for iron(II) complexes with nitrogen donor atoms. Currently, about two hundred spin transition systems are known.

The SCO phenomenon has been studied by a variety of physical methods such as magnetic susceptibility and heat capacity measurements, Mössbauer, Raman, UV/Vis, IR and EPR spectroscopy and also X-ray diffraction and dielectric constant measurements.[1,2] These methods combined with temperature, pressure, high magnetic field and light irradiation provided a firm basis for the theoretical modelling of the SCO. In our group (Toulouse, France) we are particularly interested in the application of an external perturbation in the macroscopic metastable states of SCO materials leading to an irreversible switching of their magnetic, optical and electrical properties. Experiments under different external stimuli will be discussed in the second part of this paper together with a theoretical treatment of experimental data.

Concerning synthetic methods, two approaches are currently employed for designing new cooperative SCO systems, namely supramolecular and polymeric approaches. These two strategies will be illustrated in the third part of the paper using several examples of mononuclear and polymeric compounds recently synthesised at ENS Lyon (France).

2. Switching of Spin States by External Perturbations

The SCO phenomenon is one of the most spectacular examples of molecular bistability which means that SCO molecules may exist in two different electronic states within a certain range of external perturbations.[7] Most notably, the existence of a thermal hysteresis in certain SCO complexes (in the solid state) confers a memory effect on these systems. This bistability is accompanied by a marked change in various physical properties. Besides the well-known magnetic and optical responses, we have recently shown that the dielectric constant can also be used to read the state of the bistable system[8] leading to the first prototype of an electronic component for information storage.[9]

According to the pioneering ideas of O. Kahn, several compounds have been designed for which room temperature falls within the hysteresis loop.[10] Using local warming and cooling for writing and erasing, O. Kahn and his colleagues have promoted devices based on SCO materials for different applications such as temperature sensors and active elements in displays and memory devices.[7] In our group, we have pursued these ideas and proposed the use of pulsed perturbations in the hysteresis loop temperature range (macroscopic metastable states) to switch the spin state of the system (Figure 1). In the first experiments we used a pulsed magnetic field to trigger an LS → HS transition.[11] Later, we showed that a pressure pulse leads to a "mirror effect" when compared with a pulsed magnetic field.[12] Recently, other groups reported the first results of the application of a laser pulse in the hysteresis loop.[13] In this chapter we discuss the effect of different external perturbations (temperature, magnetic field and pressure) on the spin state of SCO materials from an experimental and theoretical point of view. A brief summary of light pulse induced effects completes this part. Finally, an example is given to illustrate the response functions (optical, magnetic and electric) associated with the bistability.

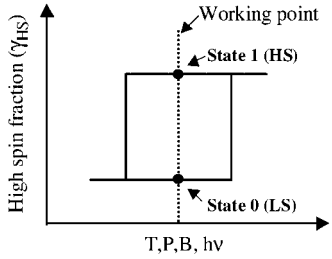

Figure 1. Schematic representation of the memory effect; the switching may be obtained by temperature, pressure, magnetic field or light irradiation

2.1. Thermally Induced Spin State Change

The thermally induced spin state change is the oldest spin-switching channel so far discovered in the field of molecular SCO compounds. The thermal spin transition curves, i.e. plots of HS fraction (γ_{HS}) vs. temperature, may take different forms such as gradual, abrupt or two-step and with or without hysteresis (see part 3 of the paper for examples). Several phenomena contribute to this different kind of behaviour, the most important being the interactions between the SCO molecules. The microscopic origins of the cooperative interactions have been extensively studied in the past and it is now generally accepted that the main contribution arises from elastic interactions between the molecules undergoing spin change. A detailed treatment of the elasticity theory was given by Spiering et al.[14]

To describe the thermally induced spin state change, in 1992 we adapted the Wajnflasz and Pick model[15] to a two-level system (HS and LS levels in our case) which we called the Ising-like model.[16] In our approach, a fictitious spin σ is associated with the HS and LS states for each molecule *i*. The Hamiltonian of the system is expressed as a function of the energy gap between the two levels of an isolated molecule (Δ_0) and a phenomenological parameter (J_{ij}) describing the interactions between the molecules *i* and *j*:

$$\bar{\mathbf{H}}_i = \frac{\Delta_0}{2}\bar{\sigma}_i - \sum_{j\neq i} J_{ij}\bar{\sigma}_i\bar{\sigma}_j$$

where $\hat{\sigma}$ is a fictitious spin operator with eigenvalues of +1 or −1 for the HS and LS states, respectively. Each level in this model represents an effective level including the electronic configuration and the vibrational density of states. In the mean field approximation, where the interaction energy of the neighbouring molecules is averaged as $J\langle\hat{\sigma}\rangle$:

$$\sum_{j\neq i} J_{ij}\hat{\sigma}_i\hat{\sigma}_j \rightarrow J\langle\hat{\sigma}\rangle\hat{\sigma}_i,$$

the magnetisation of the system, proportional to the mean value of $\sigma = \langle\hat{\sigma}\rangle$ is a self-consistent equation and the fraction of HS molecules takes the form:

$$\gamma_{HS}(T) = \frac{r}{r+\exp\frac{\Delta_0 - 2J(2\gamma_{HS}-1)}{k_BT}}$$

with $r = g^{HS}/g^{LS}$ being the degeneracy ratio of the HS and LS levels including the vibrational contributions. The equilibrium temperature $T_{1/2}$ (obtained for $\gamma_{HS} = \gamma_{LS} = 1/2$) takes the form:

$$T_{1/2} = \frac{\Delta_0}{k_B \ln r}$$

In the case where the cooperative interaction exceeds a critical value ($J > T_{1/2}$), one observes a discontinuity in the first derivative of the free energy F of the system, leading to a first-order spin transition. In this case we observed a hysteresis loop. By introducing two kinds of cooperative interactions, namely "ferro-like" (positive) and "antiferro-like" (negative), this model reproduces the main thermal SCO behaviour observed experimentally: one-step or two-step transitions, with or without hysteresis loops.[16] Figure 2 shows four examples of theoretically calculated curves.

It is now well established that the HS form is stabilised at higher temperatures due to its higher entropy (electronic and vibrational in origin) when compared with the LS form. The prominent role of the entropy difference between the HS and LS states (ΔS_{HL}) in driving the thermal spin crossover was first considered by Sorai and Seki.[17] These authors studied the heat capacity of the compound $[Fe(phen)_2(NCS)_2]$ as a function of temperature and found a heat capacity anomaly around the spin crossover temperature (176 K). The entropy change associated with the spin transition was then estimated to be $\Delta S_{HL} = (49.0\pm0.7)$ $J\cdot K^{-1}\cdot mol^{-1}$. Since the entropy change measured by Sorai and Seki is significantly larger than the electronic entropy change, they proposed that the main contribution to ΔS_{HL} arises from the coupling of the electronic state to the phonons of the system. In a first approach, this effect can be explained by the increase in the number of antibonding e_g electrons upon an LS → HS crossover of the central metal ion. This electronic change significantly weakens the metal−ligand bonds leading to lower vibrational frequencies. For example the metal−ligand stretching frequencies, which are those most influenced by the spin state change, were found to decrease by a factor of 1.5−1.8. In other words, the density of vibrational states shifts to the low frequency range when going from the LS to the HS state. Since the contribution of low-frequency modes to the vibrational entropy will be higher, this phenomenon leads to a more entropic HS state.

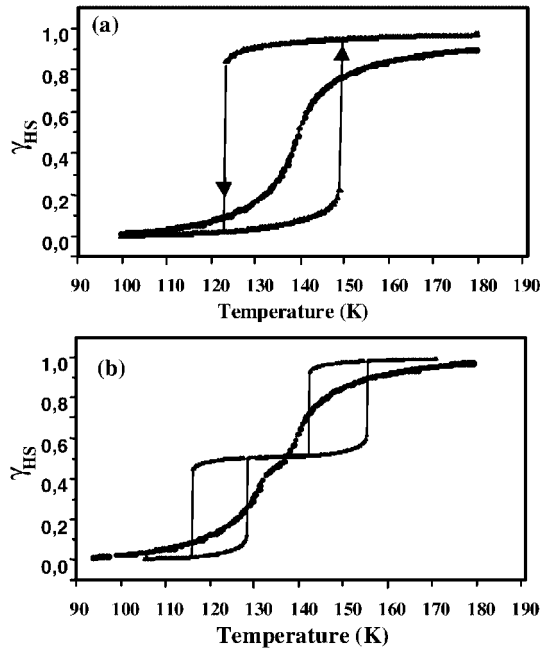

Figure 2. Calculated thermal variation of γ_{HS} using the Ising-like model: (a) one-step spin crossover: gradual ($J < T_{1/2}$) and abrupt with hysteresis loop ($J > T_{1/2}$); (b) two-step spin crossover: gradual and abrupt with two hysteresis loops

We have studied the effects of molecular vibrations on the SCO phenomenon using vibrational spectroscopic methods as experimental tools and by including the molecular vibrations in our Ising-like theoretical model.[16d,18] The vibrational spectra, even recorded by a variety of methods (Raman, IR, nuclear inelastic scattering), cannot provide the complete vibrational spectrum. For these reasons, theoretical treatments incorporating vibrational effects must inevitably rely on various approximations.

The Raman spectra of $[Fe(phen)_2(NCS)_2]$ have been analysed[18a] by making the assumption of an average frequency representative of the idealised FeN_6 octahedron. An average frequency ratio of 1.35 was obtained which is in good agreement with the result (1.5) of recent DFT calculations on the same compound.[19] Using this value, an estimated vibrational contribution to the entropy change from the coordination core of 20 $J\cdot K^{-1}\cdot mol^{-1}$ was obtained. This result supports the proposition of Sorai and Seki[17] that the intramolecular vibrations represent a prominent contribution to the overall entropy change.

The inherent limitations of the average frequency approach have been addressed by summing the entropy terms associated with the distinct vibrational modes.[18b,18c] A family of coordination polymers of formulae $[Fe(pyridine)_2(M(CN)_4)]$ and $[Fe(pyrazine)(M(CN)_4)]\cdot 2H_2O$ (M = Ni, Pd, or Pt), displaying comparatively clear-cut low-fre-

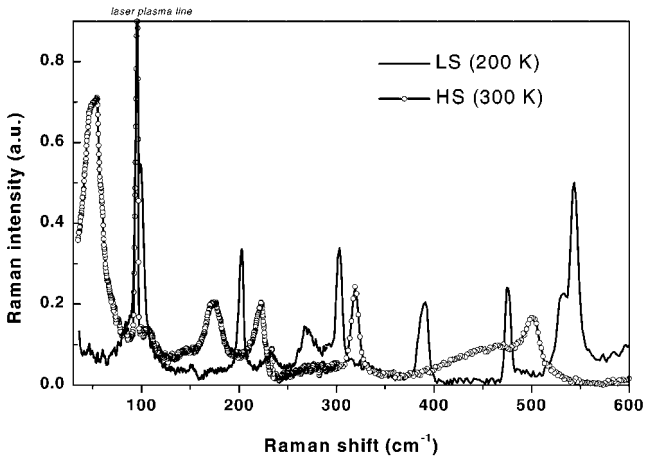

Figure 3. Raman spectra of the [Fe(pyrazine)(Pd(CN)$_4$)]·2H$_2$O spin crossover complex in the HS (300 K) and LS (200 K) states[18c]

quency vibrational spectra (Figure 3), has recently been studied by using this approach.[18c] It was shown that the spin state change in these compounds influences not only the vibrations which can be described as Fe^{II}−ligand modes but all other low-frequency modes of the polymeric network (below ca. 600 cm^{-1}). It was concluded that alongside a major contribution from the metal−ligand vibrations (ca. 60 %) other intra- and intermolecular vibrations can also make nonnegligible contributions to the entropy change (ca. 40 %). The underlying reason may involve either coupling with the Fe^{II}−ligand vibrations or with the lattice contraction/expansion that accompanies the spin transition. High pressure,[18f] isotopic substitution[18d] and metal dilution[18g] techniques combined with Raman spectroscopy and calorimetry measurements revealed that in this family of compounds, ΔS_{HL} decreases upon isotope exchange and metal dilution but does not change much with the lattice contraction. These observations suggest, therefore, that the vibrational couplings have a significant effect on the entropy change.

Thus, both infrared and Raman spectroscopy reveal a pronounced change in the molecular vibrational modes. We have also studied theoretically the effect of intramolecular vibrations on the spin crossover phenomenon for independent molecules involving a set of harmonic oscillators.[16d] Each two-level molecule is associated with p harmonic oscillators having two possible frequencies, ω_{LS} and ω_{HS} (p = 15 for an octahedral symmetry). For each oscillator of frequency ω_i, the vibrational partition function can be written:

$$z_i(\omega_i,T) = 1/[\exp(h\omega_i/kT) - 1]$$

The contribution of oscillator (i) to the total entropy is then derived from the free energy expression ($F_i = -kT\ln z_i$; $S_i = -\partial F_i/\partial T$) leading to:

$$S_i(\omega_i,T) = h\omega_i/2T\cdot\tanh(h\omega_i/2kT) - k\cdot\ln[2\sinh(h\omega_i/2kT)]$$

The total entropy of the system can be calculated by summing the contributions of the different vibrational modes. The decrease in the frequencies upon LS → HS crossover results in an entropy increase that can be expressed by:

$$\Delta S_{HL}(T) = S_{HS}(T) - S_{LS}(T)$$

The frequency dependence of the contribution of a given mode on the total entropy change calculated according to the above equations is shown in Figure 4 at different temperatures. The higher the frequency and the lower the temperature, the less the mode contributes to $\Delta S_{HL}(T)$.

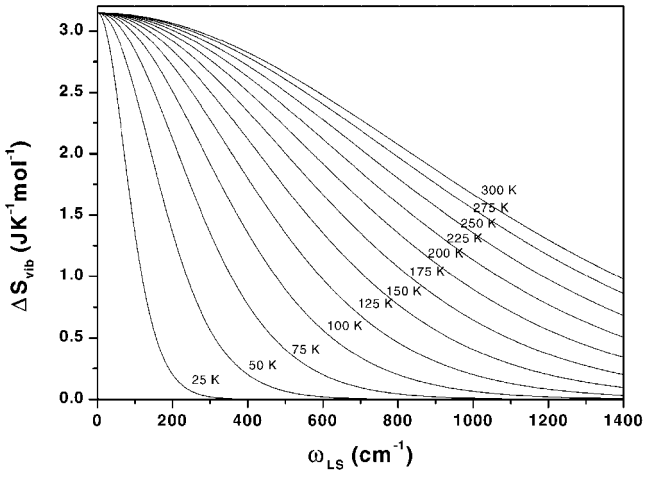

Figure 4. Vibrational entropy change of a harmonic oscillator upon spin transition as a function of the vibrational frequency; the curves were calculated with $\omega_{HS} = \omega_{LS}/1.5$ for different values of T_c [18c]

Interesting behaviour occurs due to the intramolecular vibrations when the system is in an "equi-energetic" situation. This situation corresponds to the case where $\Delta_{eff} = \Delta_{elec} - p\bar{h}(\omega_{LS} - \omega_{HS})/2 \approx 0$, i.e. when the contribution of the molecular vibrations is of the same order of magnitude as the electronic gap between the HS and LS states. In this case, the HS state will be the ground state at low temperature and one may observe, as illustrated in Figure 5, a partial SCO phenomenon with particular thermal behaviour.[16d] To date, three examples of such "equi-energetic" situations have been reported,[20] the first two examples coming from our group in 1996 and 1998.

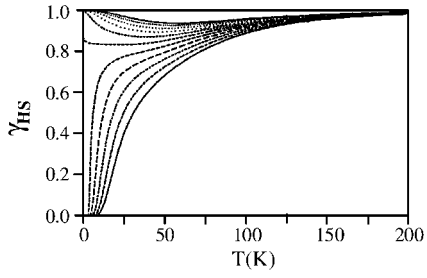

Figure 5. Theoretical thermal variation of γ_{HS} in the vicinity of the "equi-energetic" (HS, LS) situation ($\Delta_{eff} = \Delta_{elec} - p\bar{h}(\omega_{LS} - \omega_{HS})/2 \approx 0$)[16e]

2.2. Magnetic Field Induced Spin State Change

Keeping in mind that (i) a magnetic field stabilises the highest spin-state of the molecule through the Zeeman effect, (ii) the spin crossover phenomenon is a dynamic process and (iii) it is possible to generate high pulsed magnetic fields[21] (LNCMP/CNRS, Toulouse, France: 32 Tesla in 2000 and 60 Tesla currently), the idea of applying a pulsed magnetic field in the hysteresis loop was developed.

Historically, the first study using a static magnetic field of 5.5 Tesla, reported by Y. Qi et al. on $[Fe(phen)_2(NCS)_2]$, revealed a shift of the thermal spin transition by −0.12 K.[22] In the second study with cobalt complexes under a static field of 20 Tesla, J. Lejay et al. measured a shift of $T_{1/2}$ by −0.6 K.[23a] In 2000, we reported the first study of the effect of a high and pulsed magnetic field (32 Tesla) on the spin state of $[Fe(phen)_2(NCS)_2]$ and a partial triggering of the SCO was demonstrated with at least a 15 % HS fraction created in an irreversible process (Figure 6).[11a]

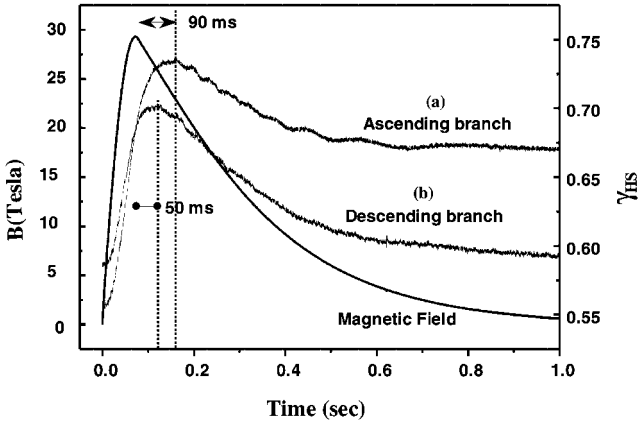

Figure 6. Magnetic pulse effect on $Fe(phen)_2(NCS)_2$; the time dependencies of $\gamma_{HS}(t)$ for two initial states belonging to the ascending (a) and descending (b) branches of the thermal hysteresis loop; for comparison, the time dependence of the magnetic field pulse is also shown[11a]

In a quasi-static approach, we modelled the observed effects under a magnetic field introduced in the Ising-like model.[11e] The magnetic field, through the Zeeman effect, removes the electronic degeneracies of the HS and LS levels and the new Hamiltonian can be written as:

$$\hat{\mathbf{H}}_i(m_S) = \frac{\Delta_0}{2}\hat{\sigma}_i + \sum_{j\neq i} J_{ij}\hat{\sigma}_i\hat{\sigma}_j + g_L\mu_B B\hat{S}_Z\frac{\hat{\sigma}_i+1}{2}$$

where μ_B is the Bohr magneton, g_L is the Landé factor, B is the magnetic field strength and S_z is the projection of the spin moment operator along the field direction. The latter can take any of the $2S + 1$ values $m_S = -S, -S + 1, ..., S$. The system can now be described by its spin state σ_i and also by m_S. In order to solve analytically the Hamiltonian of the system, we use the mean-field approximation. By explicit calculation of the mean value of $\hat{\sigma}$ we obtain for γ_{HS}:

$$\gamma_{HS}(B) = \frac{r(B)}{r(B)+\exp\frac{\Delta_0 - 2J(2\gamma_{HS}-1)}{k_BT}}$$

$$with \quad r(B) = \frac{g_{HS,vib}\,g(B,S_{HS})}{g_{LS,vib}\,g(B,S_{LS})} \quad and \quad g(B,S) = \frac{\sinh\left(\frac{(2S+1)g_L\mu_BB}{2k_BT}\right)}{\sinh\left(\frac{g_L\mu_BB}{2k_BT}\right)}$$

and for $T_{1/2}$:

$$T_{1/2} = \frac{\Delta_0}{k_B\ln\left\{\frac{g_{HS,vib}}{g_{LS,vib}}\cdot\frac{\sinh\left[\frac{(2S_{HS}+1)g_L\mu_BB}{2k_BT_{1/2}}\right]}{\sinh\left[\frac{(2S_{LS}+1)g_L\mu_BB}{2k_BT_{1/2}}\right]}\right\}}$$

where $g_{HS,vib}$ and $g_{LS,vib}$ are the vibrational degeneracies of the HS and LS states, respectively.

The exact solution of these self-consistent equations can only be obtained numerically. Figure 7 represents the resolution of the $\gamma_{HS}(T,B)$ equation using the Newton numerical method. This resolution was carried out in the case of a gradual conversion between the diamagnetic ($S_{LS} = 0$) and the paramagnetic ($S_{HS} = 2$) spin states with the parameter set as $\Delta_0 = 700$ K, $J = 139$ K, $g_{HS,vib}/g_{LS,vib} = 30$ and for different strengths of the applied magnetic field. It can be noted that for an applied magnetic field above 18 T, a first-order phase transition appears accompanied by a thermal hysteresis. This effect has also been shown qualitatively in ref.[23b] In fact, the magnetic field decreases the transition temperature but the condition for a first-order transition $J/k_BT_c > 1$ remains unchanged. This condition is illustrated in Figure 8, where, for $J = 139$ K, the first-order phase transition appears above 18 T.

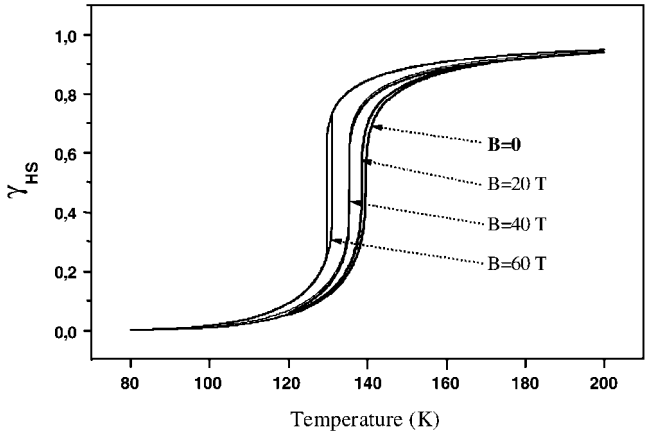

Figure 7. Calculated thermal variation of $\gamma_{HS}(T,B)$ under a static magnetic field using the Ising-like model,[11e] for selected values $B = 0$, 20 T, 40 T and 60 T; a thermal hysteresis loop (first-order phase transition) is obtained for $B = 60$ T

As described in ref.[11a] we can also obtain an analytical expression for the variation of $T_{1/2}$ as a function of the applied magnetic field strength from the Landau free energy in the presence of a field and in thermodynamic equilibrium. For an isothermal process and in the high-temperature approximation (paramagnetic Curie law), the magnetic molar free energy can be written as:

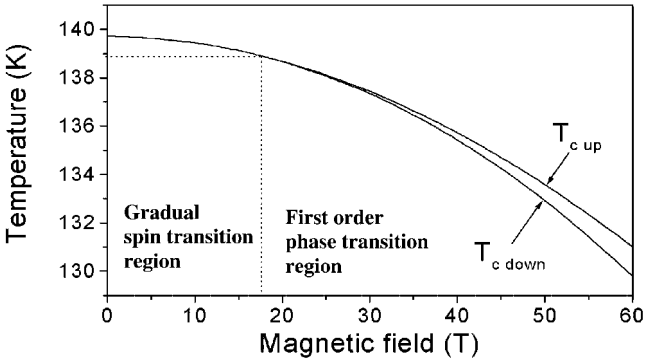

Figure 8. (B,T) phase diagram calculated using the Ising-like model (with $S_{LS} = 0$, $S_{HS} = 2$, $\Delta_0 = 700$ K, $J = 139$ K, $g_{HS,vib}/g_{LS,vib} = 30$)[11e]

$$\Delta G = G_{HS} - G_{LS} = \Delta H(0) - T\Delta S(0) - (\chi_{HS} - \chi_{LS})B^2/2\mu_0$$

where $\Delta H(0)$ and $\Delta S(0)$ refer to the properties in the absence of an external field. Accounting for the paramagnetic properties of the HS state, for a spin $S = 0 \rightarrow S = 2$ transition we obtain:[11a,11g]

$$\delta T_{1/2} = -\frac{4(\mu_B B)^2}{k_B \Delta_0}$$

and

$$\delta(\Delta) = \Delta(B) - \Delta(0) = -4(\ln g)(\mu_B B)^2/\Delta(0)$$

For a spin crossover between two paramagnetic states ($S = 1/2 \rightleftarrows S = 3/2$) the equilibrium temperature shift takes the form:[11d,11e]

$$\delta T_{1/2} = -\frac{2(\mu_B B)^2}{k_B \Delta_0}$$

The negative sign for both the equilibrium temperature and the energy gap between the HS and the LS states due to coupling to the magnetic field leads, as expected, to the stabilisation of the HS form.

Newton numerical resolution of $T_{1/2}$ obtained in the Ising-like model has been described in ref.[11e] It appears, as expected, that the transition temperature decreases quadratically with the magnetic field B and the two approaches (Ising-like and thermodynamic) are equivalent for weak magnetic fields but diverge for strong fields.

The dynamic aspects of the pulsed magnetic experiments are very interesting. In Figure 6 the peak value of the applied magnetic field (32 T) corresponds to a computed shift of the transition temperature $\Delta T_{1/2} \approx -1.8$ K which is sufficient for a complete triggering to be expected in the quasi-static regime. Therefore, the incompleteness of the spin switch can be associated with the kinetic part of the pulsed field experiment.

Subsequently, using the metal-diluted complexes $Fe_xNi_{(1-x)}(btr)_2(NCS)_2 \cdot H_2O$ [btr = 4′,4′-bis(1,2,4-triazole)], we observed a clear correlation between the cooperativity of the thermal transition and the dynamics of the triggering process. In particular, the delay between the excitation (magnetic pulse maximum) and the response increases exponentially with increasing cooperativity (J) (Figure 9).[11c,11f]

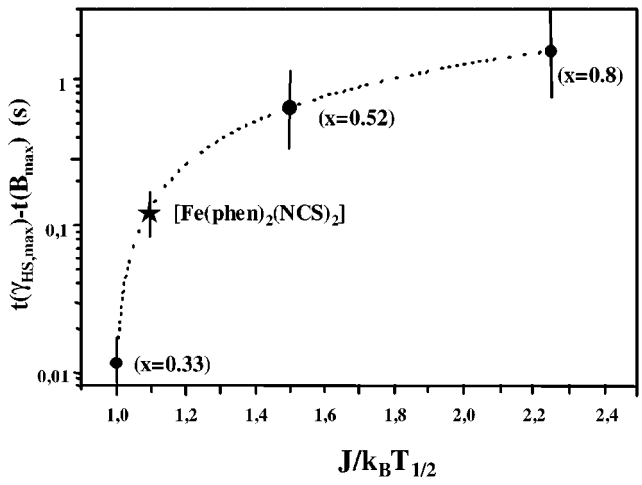

Figure 9. The time delay between $B^{max}(t)$ and $n_{HS}^{max}(t)$ on the ascending branch of the hysteresis loop (for initial temperatures corresponding to a molecular fraction $\gamma \cong {}^0_{HS} = 0.4$) for different samples of $[Fe_xNi_{(1-x)}(btr)_2(NCS)_2]\cdot H_2O$ mixed crystals as a function of J/k_BT_c;[11c] the point obtained with $Fe(Phen)_2(NCS)_2$ is also reported[11a]

This work prompted us to study, under a magnetic field, a system with a low energy barrier between the (macroscopic) LS and HS states and with a paramagnetic LS state in order to observe a complete spin-state switching. For this aim we selected the compound $Co^{II}[H_2(fsa)_2en](py)_2$.[11d] As shown in Figure 10, applying a magnetic field of 32 T to this system, initially being in the ascending branch of the hysteresis loop, leads to an irreversible and quasi-complete $S = 1/2 \rightarrow S = 3/2$ transition.

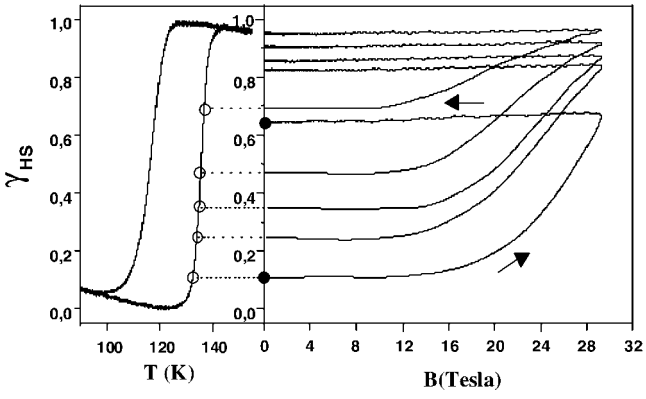

Figure 10. Magnetic pulse effect on $[Co\{H_2(fsa)_2en\}(py)_2]$; set of isotherms $\gamma_{HS}(T,B)$ showing the irreversible triggering of the LS → HS transition for an applied pulsed magnetic field in the ascending branch of the hysteresis loop;[11d] the pathway of the increase in the proportion of high-spin molecules as function of magnetic field is shown by the arrows

The kinetic aspects of the spin crossover triggering by pulsed magnetic fields were modelled through dynamic treatments of the Ising-like model.[11d] This requires a stochastic description based on the following master equation:

$$\frac{d}{dt}p(\{\sigma\},t) = \sum_j W_j(-\sigma_j)p(\{\sigma_j\},-\sigma_j;t) - \sum_j W_j(\sigma_j)p(\{\sigma_j\},\sigma_j;t)$$

where $p(\{\sigma\},t)$ is the probability of observing the system in the configuration $\{\sigma\} = (\sigma_1, \sigma_2, ..., \sigma_N)$ at time t and $\{\sigma\}_j$ denotes the configuration of all spins, except σ_j. $W_j(\sigma_j)$ which are the transition rates of the spin flip $\sigma_j \rightarrow -\sigma_j$, induced by the thermal bath which are constrained in order to respect the microscopic detailed balance condition.

In the mean-field approximation, we obtained the following nonlinear differential equation for the HS fraction of molecules $\gamma_{HS} = (1 + m)/2$:

$$\frac{d\gamma_{HS}}{dt} = -\frac{2}{\tau_0}\gamma_{HS}e^{-\beta\varepsilon^+}e^{-2\beta qJ\gamma_{HS}} + \frac{2}{\tau_0}(1-\gamma_{HS})e^{-\beta\varepsilon^-}e^{2\beta qJ\gamma_{HS}}$$

$$\text{with } \varepsilon^{\pm} = \pm E_a^0 \mp \frac{\Delta_0}{2} \mp qJ \pm \frac{kT}{2}\ln 2\frac{g_{HS}}{g_{LS}} \pm 2\frac{(\mu B(t))^2}{kT}.$$

Figure 11 represents the solution of the equation for $\gamma_{HS}(t,T)$ in the ascending and descending branches of the thermal hysteresis loop: this model is (i) qualitatively in good agreement with the experimental behaviour and (ii) reproduces the nonreversible/reversible character of the triggering in the ascending/descending modes, respectively.

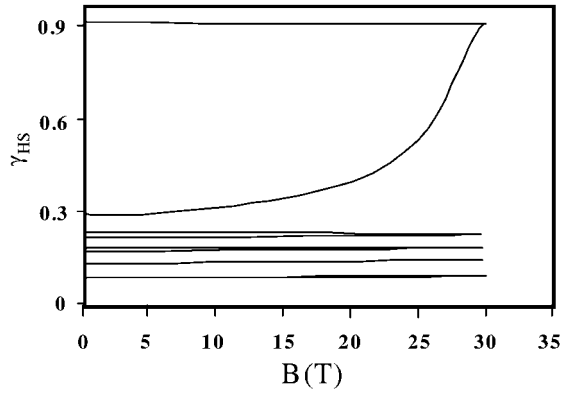

Figure 11. Calculated HS fraction as a function of the pulsed magnetic field B in the ascending branch of the hysteresis loop;[11d] no significant effects of magnetic field are observed for initial values of $\gamma_{HS} < 0.3$ (lower section of the figure)

As a summary of the main findings associated with the effects of intense and pulsed magnetic fields we refer to the following points:

1. In the first experiments with $Fe(phen)_2(NCS)_2$:[11a]

a) In the ascending (metastable) branch of the thermal hysteresis loop, a partial irreversible triggering of the spin crossover was obtained (15% of the LS molecules) by applying a 32 T pulsed magnetic field. In other words, in the ascending branch we succeeded in triggering the "first-order" (in the nonequilibrium sense) magnetic field induced spin transition.

b) In contrast to the situation with the ascending branch, reversible triggering was obtained in the descending branch (i.e. in this branch, the system cannot reach a metastable state in a magnetic field.)

c) Dynamic effects of the phenomenon are evidenced by the delay between the excitation (application of magnetic field) and the response (increase of high spin fraction) measured at 50 ms and 90 ms for the ascending and descending branches of the thermal hysteresis loop, respectively.

2. In a second series of experiments with the $Fe_xNi_{(1-x)}(btr)_2(NCS)_2{\cdot}H_2O$ family of complexes:[11c]

a) Similar effects were obtained with $x = 0.33$, 0.52, 0.8 in the ascending/descending branches of the hysteresis loops.

b) The delay between the excitation and the response increased exponentially with increasing cooperativity.

3. In a third series of experiments on $[Co(H_2(fsa)_2en)py_2]$, a quasi-total triggering of the SCO was observed[11d] and was attributed to the low energy barrier ($\Delta = 442$ cm^{-1}) between the HS and LS forms and to the paramagnetic character of the LS state ($S = 1/2$).

4. A dynamic Ising-like model, including a magnetic field, reproduced well the experimental observations.[11d]

2.3. Pressure-Induced Spin State Change

The LS → HS spin state change of the central metal ion in a molecule brings about a significant increase in the metal−ligand bond lengths and, as a result, an increase of the unit cell volume. This volume change associated with the SCO may reach several percent of the unit cell volume in iron(II) complexes as determined from X-ray diffraction data.[1,2] In the case of complexes with an $Fe^{II}N_6$ core, ΔV_{HL} is typically around 20 Å^3/iron atom.[24k,24l]

Externally applied pressure stabilises the LS state (i.e. with a smaller volume). Pressure thus has the effect of shifting the thermal spin transition towards higher temperatures.[24] It also speeds up the relaxation back to the LS state at a given temperature.[24g−24i,25a] For complexes with an $Fe^{II}N_6$ core, the shift in the transition temperature was found, in general, to be around 15 K/kbar, though in certain cases a few exceptions were also found.[24e,24f,24k]

The pressure effects on the SCO can be modelled within the Ising-like model using the mean-field approximation and by taking into account only a direct coupling between the HS fraction and the pressure through the work term which increases the energy gap ($\Delta_p = \Delta_0 + p\Delta V_{HL}$).[11g,24j,25] In this case the shift of the transition temperature with pressure is given as:

$$\delta T_{1/2}/\delta p = \Delta V_{HL}/\Delta S_{HL}$$

where ΔS_{HL} is the total entropy change upon SCO and ΔV_{HL} is the volume change. The positive sign of both ΔS_{HL}

and ΔV_{HL} leads to a positive shift of $T_{1/2}$ with increasing pressure.

In the case of a first-order phase transition, the spin crossover is usually accompanied by a hysteresis loop. The hysteresis loop can be obtained from the Ising-like model if the condition $J > T_{1/2}$ is fulfilled.[16] The surface of the hysteresis loop is proportional to the difference between the cooperativity of the system and the equilibrium temperature [$S \sim (J - T_{1/2})$].[26] The positive sign of the shift of the equilibrium temperature obtained by the Ising-like model thus leads to a vanishing of the hysteresis loop upon increasing pressure.

The pressure-induced spin switching around room temperature can be illustrated by the example of the polymeric spin crossover compound $[Fe(Atrz)_3](NO_3)_2 \cdot nH_2O$ (Atrz = 4-amino-1,2,4-triazole). Mössbauer spectroscopic measurements have been carried out under pressure at 325 K, i.e. in the temperature range of the thermal hysteresis loop of this compound. Figure 12 shows Mössbauer spectra of this complex obtained at 325 K at low pressure (50 bar), under compression (1000 bar) and after decompression (50 bar). At low pressure the spectrum consists of a main doublet (80 %) with hyperfine parameters characteristic of Fe^{II} in the HS state (IS = 1.00 mms^{-1}, QS = 2.54 mms^{-1}) and a small (20 %) doublet (IS = 0.41 mms^{-1}, QS = 0.14 mms^{-1}) which can be assigned to LS Fe^{II} species. By application of 1000 bar, the system can be converted completely to the LS state as shown by the Mössbauer spectra. Since at the temperature of the experiment the system is in the hysteresis region of the phase diagram, after decompression it remains in the LS state, i.e. the piezo-switch is irreversible.

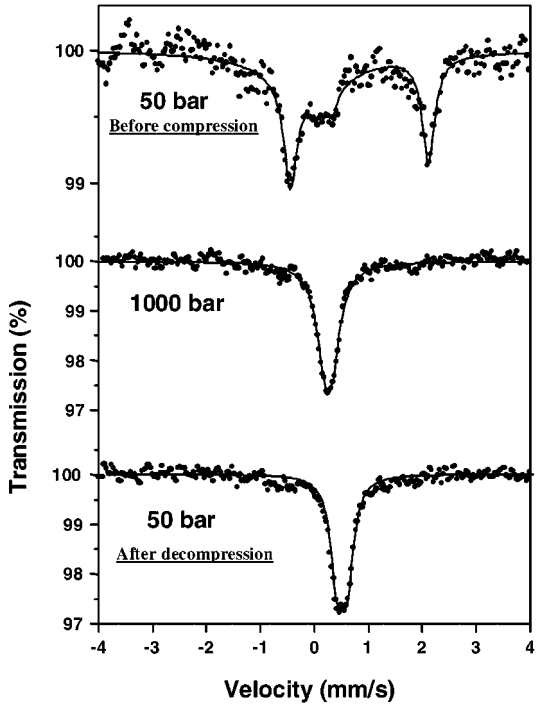

Figure 12. Pressure-induced spin switching in $[Fe(Atrz)_3](NO_3)_2 \cdot nH_2O$ at 325 K detected by Mössbauer spectroscopy

Since the early stages of SCO research, several authors have discussed interest in the influence of pressure on SCO systems.[24] However, pressure effects on these molecular materials have been found to be relatively complex. For example, pressure was often found to induce changes in the crystal structure.[27] For this reason, we decided to probe the pressure effects on SCO systems using a spectroscopic technique (Raman spectroscopy).

The spin states of a series of cyanide-bridged iron(II) spin-crossover coordination polymers of formulae $Fe(pyrazine)[M(CN)_4] \cdot 2H_2O$ (M = Ni, Pd, or Pt) have been studied by recording their solid state Raman spectra at room temperature as a function of pressure (Figure 13).[25b] For the first time, a reproducible piezo-hysteresis loop has been observed at room temperature for the Ni complex with characteristic spin transition pressures of $P_{1/2}\uparrow$ = 1350 bar and $P_{1/2}\downarrow$ = 650 bar upon compression and decompression, respectively. The fascinating feature here is the use of a perturbation other than the temperature to obtain a memory effect (piezo-hysteresis loop). Using the Ising-like model described above, we simulated piezo-hysteresis curves and we were able to show that the condition required to obtain a discontinuous pressure loop can be written as $J > T_{1/2}(p = 0) + P_{1/2}\Delta V(p)/\Delta S(p)$. Since the second term is always positive, piezo hysteresis can be expected only for complexes displaying thermal hysteresis at atmospheric pressure. Moreover, the piezo-hysteresis vanishes with increasing temperature (Figure 14). For the Pd and Pt complexes, the spin-state change occurs at higher pressures (1.8 and 3.5 kbar, respectively) and without hysteresis. The unexpectedly high value of $P_{1/2}$ in the case of the Pt complex was puzzling but Raman spectroscopy revealed that in this complex, a structural phase transition takes place at relatively low pressures (100−900 bar). The pressure-induced phase could be identified as a low-symmetry HS phase. This new HS phase transforms to the LS form only at higher pressures.

Using Raman spectroscopy in conjunction with a diamond anvil cell technique, a spin state change for the complex $Fe(pyridine)_2[Ni(CN)_4]$ could be observed at around

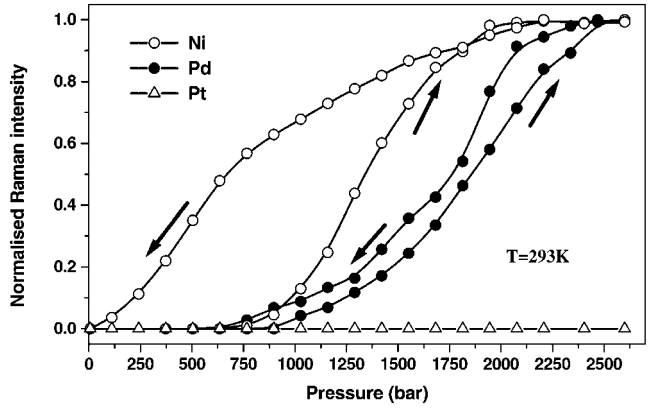

Figure 13. Intensity of the 675 cm^{-1} LS marker band as a function of pressure for the complexes $Fe(pyrazine)[M(CN)_4] \cdot 2H_2O$ (M = Ni, Pd, or Pt) at room temperature (arrows indicate the increase and subsequent decrease of the pressure)[25b]

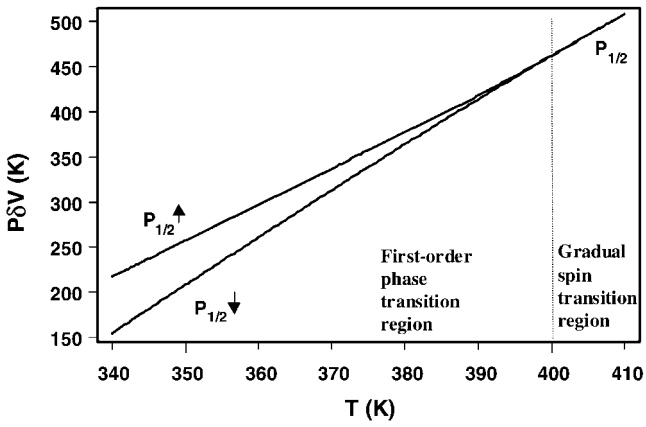

Figure 14. Calculated (P,T) phase diagram using the Ising-like model (with $g_{HS}/g_{LS} = 100$, $\Delta = 1380$ K, $J = 400$ K)[25b]

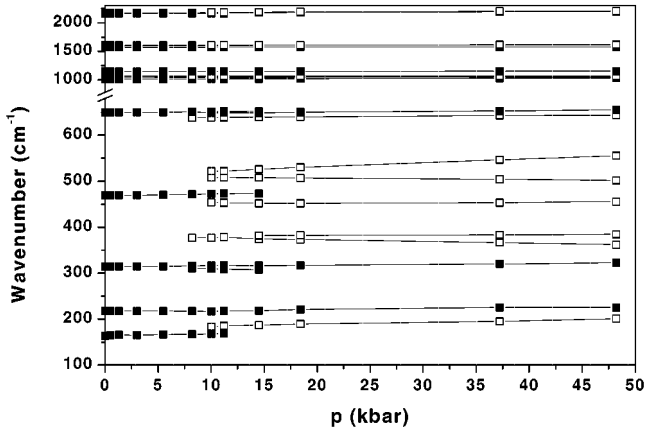

Figure 15. The pressure dependence of Raman frequencies in Fe(pyridine)$_2$[Ni(CN)$_4$]; symbols: black squares/open squares represent modes assigned to the HS/LS phase, respectively; lines are inserted to guide the eye[18f]

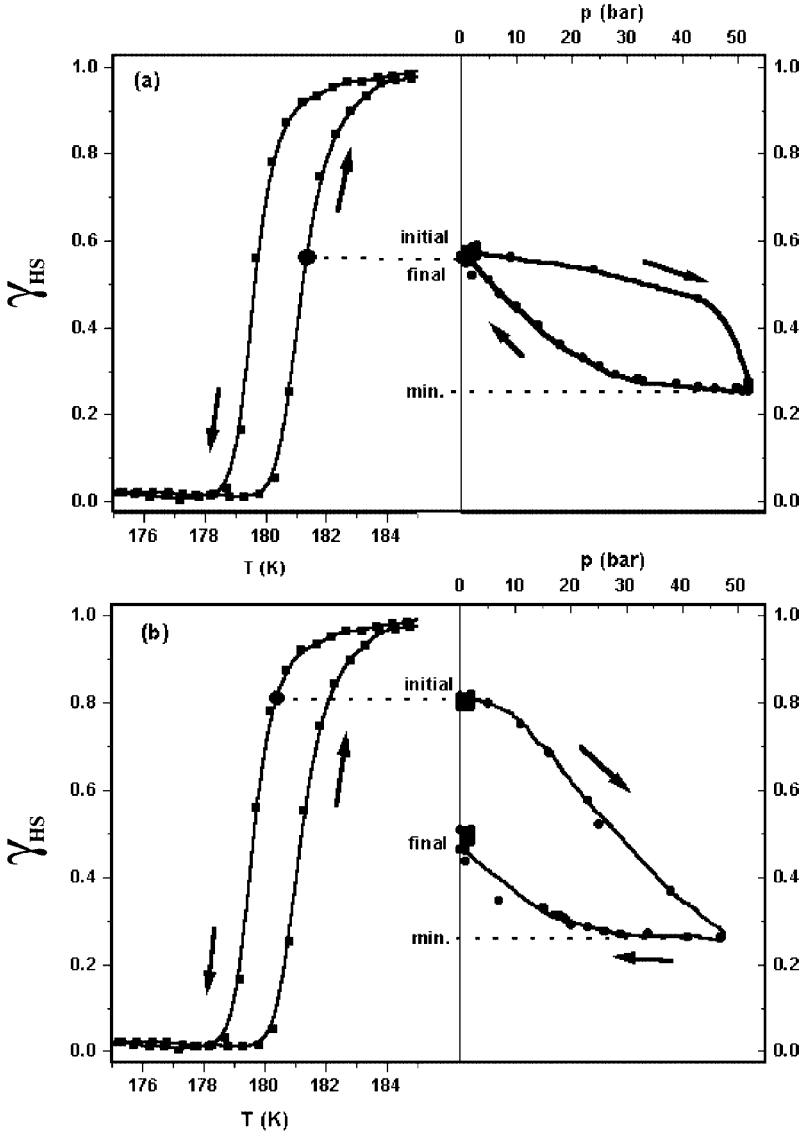

Figure 16. Pressure effect on the HS fraction $\gamma_{HS}(T,p)$ in Fe(phen)$_2$(NCS)$_2$ in the ascending (a) and descending (b) branches of the thermal hysteresis loop[12]

10 kbar.[18f] The aim of this work was to study the effect of the lattice contraction on the vibrational frequencies in the HS and LS states, generated by externally applied pressure up to 50 kbar. This question has already been brought up in several previous European discussions (TOSS network) and in theoretical investigations.[16d,28] In fact, the expansion/contraction of the lattice upon spin crossover must induce a vibrational entropy change due to the anharmonicity of vibrations. In general, this pressure-induced entropy change is neglected in the treatment of the free energy of the system, though no experimental data are available. We have determined the pressure coefficients ($d\omega/dp$) of vibrational modes in $Fe(pyridine)_2[Ni(CN)_4]$ in both the HS and LS states down to 150 cm^{-1} (Figure 15). The pressure dependence of the Raman modes was found to vary between 0.1 and 0.4 $cm^{-1}\cdot kbar^{-1}$ in the investigated frequency range for both HS and LS frequencies. We therefore concluded that at moderate applied pressures ($< 10-15$ kbar) the lattice contraction induced entropy change is small and can be in fact neglected.[18f]

Besides the static effects of pressure on the SCO we have also studied the effects of a pressure pulse in the temperature range of the thermal hysteresis loop for the compound $Fe(phen)_2(NCS)_2$.[12] During the dynamic pressure pulse, a decrease in γ_{HS} can be observed with an irreversible (reversible) character in the descending (ascending) branch of the hysteresis loop (Figure 16). In this respect, pressure has a "mirror effect" compared with the application of an intense and pulsed magnetic field for which an increase in γ_{HS} is observed with an irreversible (reversible) character in the ascending (descending) branch of the hysteresis loop. This observation can be explained by the fact that an applied magnetic field stabilises the HS state through the Zeeman effect while external pressure stabilises the LS state due to its smaller volume. If one compares the theoretical shift of the transition temperature under quasi-static external pressure with that due to a magnetic field, it appears that the effect of 1 T is roughly the opposite of the shift caused by 2.5 bar. The fact that a pressure as low as 200 bar triggered a complete crossover between the two spin-states suggests that piezo effects might be implemented in devices for addressing SCO materials (e.g. pressure sensors).

2.4. Light Pulse Induced Spin State Change

A photo-induced technique for the study of SCO in Fe^{II} complexes was first reported by McGarvey and Lawthers in 1982 in a paper describing the use of a pulsed laser to perturb the equilibrium between the singlet (^1A) and quintuplet (^5T) states in several Fe^{II} complexes in solution.[29] Then, in 1984, Descurtins et al. reported that light irradiation of a solid Fe^{II} spin crossover complex at low temperature induced a transition from the LS to a metastable HS state.[30] Subsequently, this so-called Light-Induced Excited Spin-State Trapping (LIESST) effect was intensely studied by Hauser et al. and its main elements are considered today to be well understood.[31] Though the LIESST effect is potentially interesting for use in optical devices, the low relaxation temperatures of the metastable HS species strongly limits such applications.[32]

On the other hand, recent reports suggest that it is possible to realise a photoinduced spin-state change at relatively high temperatures when exciting the solid material with a short laser pulse in the thermal hysteresis loop region. This phenomenon was first demonstrated on the complex $Fe(PM\text{-}BiA)_2(NCS)_2$.[13a] In the hysteresis loop temperature range (around 170 K), an increase of the HS fraction was obtained using single laser pulse (5 ns, ca. 1 mJ). Similar phenomena have been reported on Prussian blue analogues exhibiting thermal hysteresis loops associated with valence tautomerism.[13b] It should be emphasised that, contrary to the LIESST effect, in these experiments the *macroscopic* metastable phase (HS or LS) is photo-transformed into the thermodynamically stable phase. It was suggested that such a phenomenon could occur if the concentration of locally photo-excited states exceeds a threshold value.

These preliminary photo-switching experiments represent interesting perspectives, especially if they prove to be effective on SCO compounds exhibiting hysteresis around room temperature. However, further experiments and theoretical work are necessary to confirm the origins of these observations.

2.5. The Promising Properties for Devices

Information processing is based on the ability to modify and retrieve a particular physical property of a material such as its electrical, magnetic or optical response. In the case of spin crossover complexes, changes of magnetic and optical properties are well documented.[1] The magnetic properties change between a paramagnetic and a diamagnetic state (Fe^{II} and Co^{III} ions) or between two different paramagnetic states (Fe^{III}, Co^{II}, Mn^{II}). The change in optical properties occurs in the visible and near-IR spectroscopic regions depending strongly on the particular complex in question. Both charge transfer (MLCT) and ligand field absorption bands contribute to these spectroscopic changes.

Though optical reading has some potential applications, it is more desirable to base these on electronic functions. In fact, the use of electronic properties offers much wider scope, particularly in the context of addressing the issue of miniaturisation through the "bottom up" (i.e. molecular level) approach. In this respect, we have recently reported results demonstrating a link between the dielectric constant and the SCO phenomenon. In fact, the real part of the dielectric constant (ε') showed a significant variation at the spin transition temperature for different iron(II) spin crossover complexes.[8] The frequency dependence of ε' was found to be negligible up to 1 MHz. As far as the origin of the dielectric constant change is concerned, one can assume to a first approximation that it results from the higher polarisability of the HS ions when compared with the LS form. Indeed, for most of the complexes, we have found a higher value of ε' in the HS state. However, in the case of the complexes $Fe[5NO_2\text{-}sal\text{-}N(1,4,7,10)]$ (sal = salicylaldehyde)

and $[Fe(bpp)_2](BF_4)_2$ [bpp = 2,6-bis(pyrazol-3-yl)pyridine], ε' decreases when going from the LS to the HS state indicating that the interpretation of these changes might be more complex especially if one considers the possible existence of crystallographic phase transitions in these compounds.

As a recent example of bistability in three properties of the same compound (magnetic, optical and dielectric) the example of $[Fe(DAPP)(abpt)](ClO_4)_2$ {DAPP = [bis(3-aminopropyl)(2-pyridylmethyl)amine], abpt = 4-amino-3,5-bis(pyridin-2-yl)-1,2,4-triazole} is shown in Figure 17. The changes in all three physical channels occur as first-order phase transitions with 10 K wide hysteresis loops centred around 176 K. The high-temperature state shows a paramagnetic Curie temperature dependence of the magnetic susceptibility, with an effective magnetic moment (μ_{eff}) of 5.5 B.M. This magnetic moment corresponds to HS Fe^{II} ions with $S = 2$. Upon cooling, μ_{eff} decreases sharply around the spin transition temperature and the paramagnetism is almost completely quenched (μ_{eff} = 0.15 B.M.) at low temperatures, in agreement with a pure diamagnetic state of Fe^{II} ions ($S = 0$). The optical reflectivity measured at 632 nm also shows hysteresis. The reflectivity is higher in the HS form indicating that the optical absorption at this wavelength is lower in this state. The dielectric constant measured at 10 kHz shows an increase of ca. 8 % upon going from the LS to the HS state. The memory effect operates around 176 K by the storage of a high or low capacitance state. No significant frequency effect has been observed on ε' in the range of 10^2-10^7 Hz.

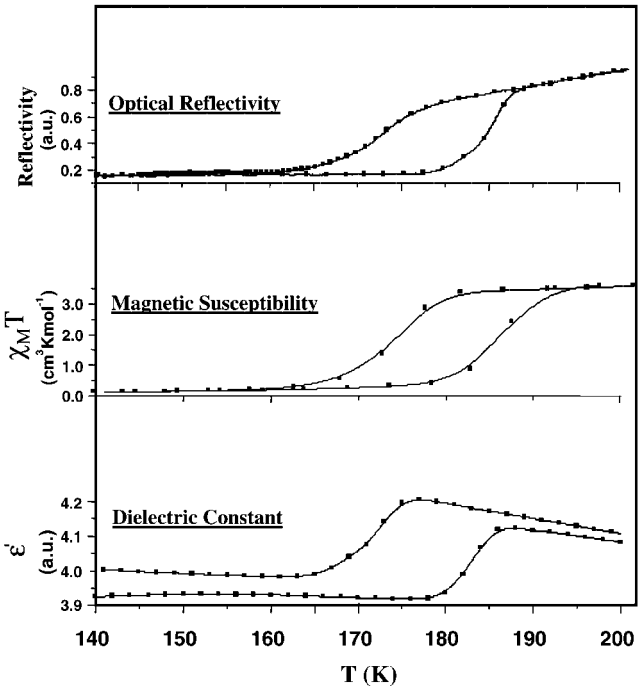

Figure 17. Thermal hysteresis loop for optical, magnetic and dielectric properties in the *same* spin crossover complex $[Fe(DAPP)(abpt)](ClO_4)_2$

3. Engineering Spin Crossover Materials

The prerequisite for the occurrence of a spin crossover is the proximity of the HS and LS electronic states. The energy gap between two states can be tuned in a relatively predictable fashion by variation of the ligand field strength. Several synthetic strategies used in the synthesis of spin transition complexes have been summarised in a recent volume of "Topics in Current Chemistry".[1] One of the possible approaches for engineering spin transition systems, applied by our group, is the use of ligands containing both aliphatic and aromatic nitrogen donor atoms. The combination of nitrogen atoms of a different nature in the same ligand can be expected to generate an intermediate ligand field, favouring spin-state interconversion. On the basis of this strategy, numerous complexes of polydentate ligands containing different types of nitrogen binding sites have been designed.[2c][2f] On the other hand, the involvement of amino and pyridyl groups in the same ligand may exert a favourable effect on the generation of intermolecular H-bonding and/or π-stacking interactions, leading to cooperative effects. Moreover, the variation of the aliphatic to aromatic nitrogen atoms ratio in the same ligand is also a convenient tool for the fine-tuning of the ligand field strength. However, the ligand field splitting is not the only factor which determines the existence and character of a spin transition. The interplay of the spin pairing energy and the ligand field strength is very sensitive to small structural perturbations in the metal environment. They may result from the existence of sterically demanding ligands and/or from minor crystal packing changes associated with the nature of the counter ions or even the presence of a solvent of crystallisation. As has been noted,[2f] even more subtle changes such as the number of chelate rings and/or the replacement of five- with six-membered cycles can also affect the spin state of the resultant iron(II) complex. Thus, in the framework of a general synthetic approach the spin transition behaviour is not generally readily predictable.

3.1. Mononuclear Complexes

In this context, in order to study the influence on the spin transition process of small perturbations in the ligand structure, several tetradentate ligands with mixed aliphatic and aromatic nitrogen atom functions were prepared (Figure 18) and their mononuclear iron(II) complexes were investigated. The new spin transition compound $[Fe(DPEA)(NCS)_2]$ [DPEA = 2-aminoethylbis(2-pyridylmethyl)amine] was isolated and its structure, magnetic properties and Mössbauer spectra were investigated.[33] This complex displays a *cis* configuration for the two NCS groups and a *mer* arrangement of two pyridyl rings of the DPEA ligand (Figure 19). The DPEA ligand, coordinated to the metal atom by two pyridine nitrogen atoms in apical positions and two aliphatic amino groups in adjacent positions in the $[FeN_6]$ octahedron, forms three 5-membered metallocycles. The X-ray analysis revealed the existence of an important distortion of the $[FeN_6]$ core from O_h symmetry, attribu-

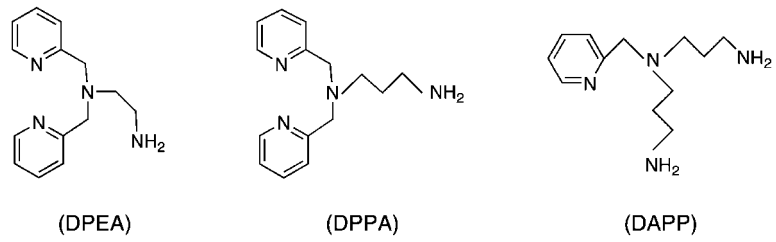

Figure 18. Representation of the DPEA, DPPA and DAPP ligands

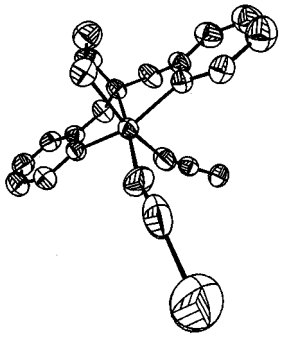

Figure 19. Molecular structure of [Fe(DPEA)(NCS)$_2$]

table to steric constraints due to the tetradentate ligand. The sharp spin conversion observed in the complex at 138 K is close to a first-order transition (Figure 20) and we anticipated that suitable changes in the structure of the ligand, which would release some strain, could modify the magnetic properties and possibly lead to a spin transition with hysteresis.

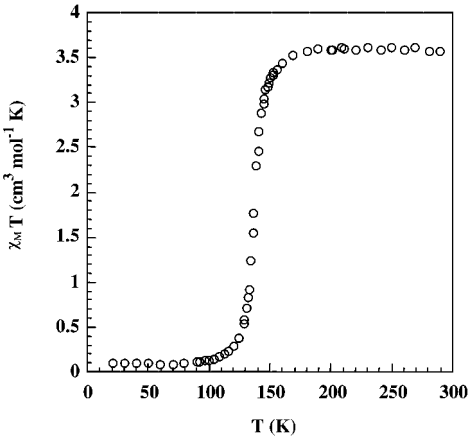

Figure 20. Thermal variation of χ_MT for [Fe(DPEA)(NCS)$_2$]

This idea was realised with the new DPPA ligand [DPPA = (3-aminopropyl)bis(2-pyridylmethyl)amine] (Figure 18) which differs from DPEA by the presence of an additional methylene unit in the amino aliphatic chain.[34] Upon coordination to iron(II), DPPA can form one 6-membered and two 5-membered chelate rings. However, during the preparation of the DPPA−iron(II) complex [Fe(DPPA)(NCS)$_2$], we isolated not a single crystalline form but four different species. Certainly, the enlargement of one of the three metallocycles leads to enhanced molecular flexibility and results in this greater variety of species. Three of these species were defined as polymorphic modifications (A, B, and C) and the fourth was a solvated complex. Only a few manifestations of polymorphism are known among spin transition systems.[35] For polymorph A, variable-temperature magnetic susceptibility measurements (Figure 21) as well as Mössbauer spectroscopy have revealed the occurrence of a rather gradual spin transition without hysteresis, centred at about 176 K. The polymorph B is paramagnetic over the temperature range 4.2−295 K, whereas polymorph C exhibits a very abrupt $S = 2 \rightleftarrows S = 0$ transition with hysteresis. The hysteresis width is 8 K, the transitions being centred at $T_c\downarrow = 112$ K for decreasing and $T_c\uparrow = 120$ K for increasing temperatures. The solvated complex [Fe(DPPA)(NCS)$_2$]·EtOH displays a rather gradual spin transition centred near 220 K. An X-ray analysis has shown that in the three polymorphs, the asymmetric units are almost identical and consist of one chiral complex molecule with the same configuration and conformation. The distorted [FeN$_6$] octahedron is formed by four nitrogen atoms belonging to DPPA and two provided by the *cis* thiocyanate groups. Contrary to our expectations, the two pyridine rings of DPPA are in the *fac* position, whereas the *mer* configuration has been isolated for [Fe(DPEA)(NCS)$_2$]. This circumstance, which made a direct comparison of the effect of metallocycle strain on magnetic properties irrelevant, offered instead a valuable opportunity to focus on the consequences of polymorphism on the magnetic properties of the same complex. The main differences between the structures of the three polymorphs are found in their crystal packings. The stabilisation of the high-spin ground state of poly-

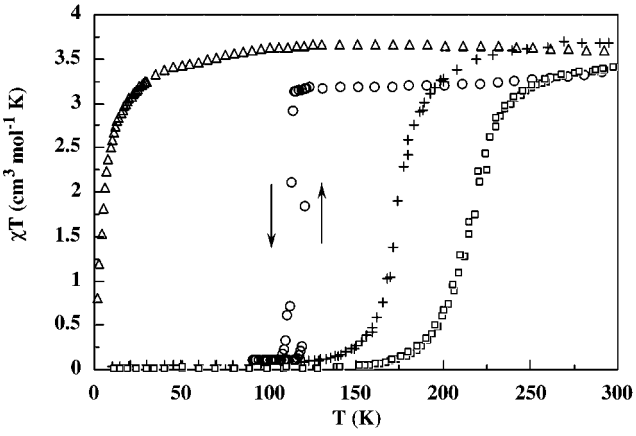

Figure 21. Thermal variation of $\chi_M T$: for *fac*-[Fe(DPPA)(NCS)$_2$] in polymorph A (+++), in polymorph B (open triangles), in polymorph C (open circles) and for [Fe(DPPA)(NCS)$_2$]EtOH (open squares)

morph B can be tentatively explained by the presence of two centres of steric strain in the crystal lattice, resulting in the elongation of the Fe−N(aromatic) distance. The observed hysteresis in polymorph C seems to be due to the existence of an array of intermolecular contacts in the crystal lattice making the spin transition more cooperative than in polymorph A. The [Fe(DPPA)$(NCS)_2$] complex provides a new and particularly striking example of polymorphism leading to qualitatively different magnetic properties in a spin transition system.

This latter example shows that the crystal structure plays a major role in the shaping of spin transitions. Packing effects appear as a small perturbation on the interplay between the ligand field and the interelectronic interactions. Besides, they determine the propagation pattern of the cooperative interactions in the solid. Unfortunately, the influence of packing effects on the spin state of the complex is neither predictable nor controllable. Another alternative, connected with the packing effects, arises when several crystallographically independent iron(II) sites co-exist in the same unit cell and structural distinctions among iron(II) complexes can result in their different magnetic behaviour.[36] This latter situation can be illustrated by the recently reported mononuclear complex [Fe(DPEA)(bim)]-$(ClO_4)_2$·$0.5H_2O$ with the DPEA ligand and bim = 2,2-bis-(imidazole).[37] Variable-temperature magnetic susceptibility measurements (77−295 K) have shown the occurrence of a two-step spin transition (Figure 22). Two steps on the magnetic curve are separated by an inflection point at 200 K, corresponding to about 50 % of the molecules having undergone a thermal spin transition. The first step is centred at 171 K and the second at 218 K. Mössbauer spectroscopy, calorimetric measurements and X-ray analyses have shown that the profile of the magnetic curve is a consequence of the presence of two nonequivalent iron(II) ions in the crystal lattice. The crystal structure was resolved in the HS and LS forms at 293 and 123 K, respectively. The main differences between both spin-state isomers were found in the geometry of the [FeN_6] core which exhibits the shorter of the Fe−N distances at lower temperatures. Two inequivalent HS molecules at two crystal lattice sites successively undergo a thermal spin transition. The attribution of the two steps of the spin transition to the inequivalent lattice sites was performed through the analysis of the mean Fe−N distances for functionally different nitrogen donor atoms. At 10 K the light-induced excited spin-state trapping (LIESST) effect was observed (Figure 23). Two critical temperatures T(LIESST) have been recorded (36 and 21 K) and attributed to the two nonequivalent iron(II) lattice sites.

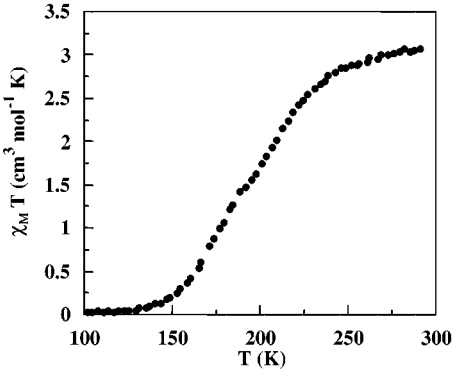

Figure 22. Thermal variation of $\chi_M T$ for [Fe(DPEA)(bim)]$(ClO_4)_2$·$0.5H_2O$

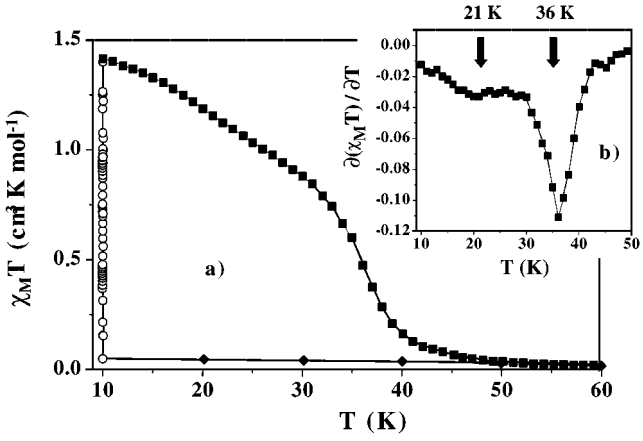

Figure 23. a) Temperature dependence of $\chi_M T$ for [Fe(DPEA)(bim)]$(ClO_4)_2$·$0.5H_2O$: data recorded in the cooling mode without irradiation (solid diamonds); data recorded with irradiation at 10 K for 2 h (open circles); data recorded in the warming mode (0.3 K min^{-1}) after the light irradiation had been applied for 2 h, then removed (solid squares); b) derivative $\partial(\chi_M T)/\partial T$

Following the study of how strain effects arising from the size of chelate rings could modify the spin-crossover regime of iron(II) complexes, the tetradentate DAPP ligand {DAPP = [bis(3-aminopropyl)(2-pyridylmethyl)amine]} (Figure 18) was then synthesised.[38] When coordinated to iron(II), DAPP can form one five-membered and two six-membered chelate rings. However, the isolated analogous complex [Fe(DAPP)$(NCS)_2$] displays only the HS state. This is certainly in line with the decrease of the ligand field strength in DAPP due to the substitution of one aliphatic nitrogen atom for an aromatic one in the DPPA ligand, resulting in an aliphatic/aromatic ratio of 3:1 in the former compared with 2:2 in the latter. Another bidentate ligand, 4-amino-3,5-bis(pyridin-2-yl)-1,2,4-triazole (abpt) was chosen to complete the octahedral coordination sphere of iron(II) and to reinforce the total ligand field strength needed for the occurrence of spin crossover. The isolated mononuclear complex [Fe(DAPP)(abpt)]$(ClO_4)_2$ displays an abrupt spin transition with a hysteresis loop of 10 K, the transition being centred at $T_c\downarrow$ = 171 K for decreasing and $T_c\uparrow$ = 181 K for increasing temperatures (Figure 24). The explanation for the pronounced cooperativity in this case was sought in the intrinsic structural features of the complex. The crystal structure was resolved in the high-spin (293 and 183 K) and low-spin (123 K) states. The X-ray analysis revealed that the cooperative spin transition results from a branched network of intermolecular interactions in the crystal lattice provided by two modes of π-stacking and numerous hydrogen bonds. The thermal spin transition is accompanied by a considerable change in the lattice param-

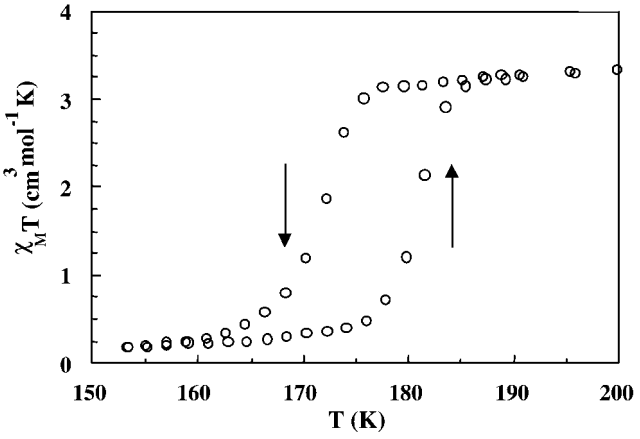

Figure 24. Thermal variation of $\chi_M T$ for [Fe(DAPP)(abpt)]$(ClO_4)_2$ in the heating mode and cooling mode

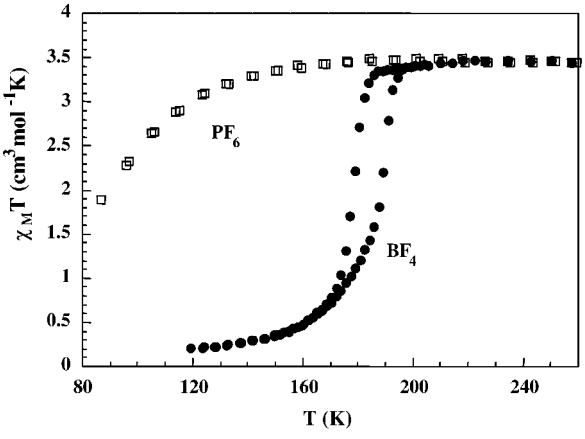

Figure 25. Thermal variation of $\chi_M T$ for (solid circles) [Fe(DAPP)(abpt)]$(BF_4)_2$ and (open squares) [Fe(DAPP)(abpt)]$(PF_6)_2$

eters (e.g. 7.5% for the *c* axis at 123 K) which in turn impose modifications on the molecular crystal packing and, accordingly, in the system of intermolecular interactions. In connection with this, the pronounced hysteresis in this complex, without any crystallographic phase transition, can be assumed to originate from the dramatic change of the unit cell parameters and rearrangement of the topology of the cooperative interactions. The second striking result of this study is the occurrence of two order-disorder transitions (in the counter anion and in the DAPP ligand) which accompany the spin change. The role of order-disorder phenomena has been discussed in the spin-crossover literature for a long time[39] and the ordering was suggested to be related to the nature of the spin transition. So far, only the disorder of species that are not coordinated to the iron(II) such as counter anions and solvent molecules, has been observed in spin transition complexes. [Fe(DAPP)(abpt)]$(ClO_4)_2$ is, to the best of our knowledge, the first example of a spin-crossover system with an order-disorder transition involving the ligand directly coordinated to the iron(II) site. In line with previous studies, the order-disorder phenomena and spin transition in [Fe(DAPP)(abpt)]$(ClO_4)_2$ seem to be internally interrelated. One may suppose that both tuning of the ligand field strength by the DAPP ligand and reinforcement of the cooperative interactions due to the thermal ordering in the perchlorate ions provide an intrinsic impulse for the initiation of the spin transition in [Fe(DAPP)(abpt)]$(ClO_4)_2$.

To examine the role of counter ions capable of giving rise to different crystal packings, we also prepared the compounds [Fe(DAPP)(abpt)]X_2 with X = BF_4, PF_6. Their magnetic behaviour (Figure 25) shows that the nature of the counter ion plays an important role in the spin-transition regime of [Fe(DAPP)(abpt)]X_2. The complex with the tetrahedral BF_4^- anion (as in the case of ClO_4^-) displays rather similar magnetic behaviour to [Fe(DAPP)(abpt)]$(ClO_4)_2$, with the hysteresis loop slightly displaced toward higher temperatures. In contrast, the complex with the octahedral PF_6^- anion shows a gradual spin transition, shifted towards lower temperatures, without hysteresis.

3.2. Coordination Polymers

The polymeric approach to designing SCO systems exhibiting strong cooperativity was only introduced quite recently[40] and therefore the number of such compounds still remains limited. The most extensively studied family includes iron(II) complexes with 1,2,4-triazole-type ligands.[41] Some of the complexes from this family, namely $[Fe(trz)_3]A_2{\cdot}nH_2O$ (trz = 4-substituted-1,2,4-triazole; A = a monovalent anion), exhibit abrupt spin transitions with a thermal hysteresis width up to ca. 40 K.[10b] The structural information for this complex has been deduced only from EXAFS spectroscopy.[42] The structure consists of linear chains in which the iron(II) atoms are triply bridged by triazole ligands. Unfortunately, structural information on the intermolecular interactions in the crystal lattice is not available. The cooperativity in these systems can be assumed to arise from a very short Fe−Fe intersite spacing and a rigid Fe−N−N−Fe linkage favouring the efficient spreading of the intersite interactions.

Several polymeric spin-crossover complexes have been synthesised using the self-assembly of rigid bifunctional N-donating spacer ligands and iron(II) ions.[20c,43] Recently, using this approach, we synthesised a new spin-crossover compound of formula $[Fe(pyim)_2(bpy)](ClO_4)_2{\cdot}2C_2H_5OH$ [pyim = 2-(2-pyridyl)imidazole and bpy = 4,4′-bipyridine].[44] It represents the first structurally characterised example of an iron(II) coordination polymer with an infinite zigzag chain undergoing the spin-crossover phenomenon. Variable-temperature magnetic susceptibility measurements revealed the occurrence of a relatively gradual spin transition centred at 205 K (Figure 26). The crystal structure was resolved at 293 K (HS form) and at 173 K (LS form). The complex assumes a 1D zigzag chain structure in which the iron(II) active sites are linked to each other by a chemical bridge such as the rigid rod-like 4,4′-bipyridine molecule. The polymeric chains which extend along the *c* axis are stacked in the *b* direction, forming 2D sheets of bound molecules (Figure 27). The sheets are linked together by several intermolecular hydrogen bonds in the *a* direction.

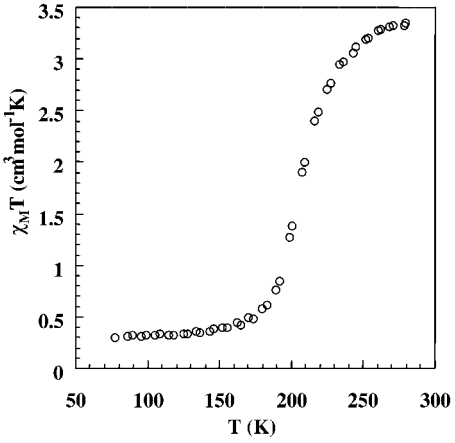

Figure 26. Thermal variation of $\chi_M T$ for $[Fe(pyim)_2(bpy)](ClO_4)_2 \cdot 2C_2H_5OH$

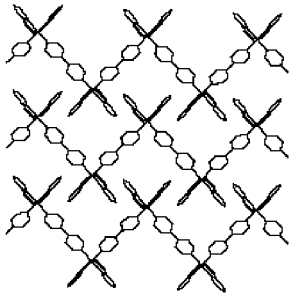

Figure 27. Projection of the molecular structure along the *a* axis for $[Fe(pyim)_2(bpy)](ClO_4)_2 \cdot 2C_2H_5OH$ showing the π−π stacking arrangement at 293 K

The ensemble of structural features of the complex, potentially leading to the cooperativity, provides a basis for strong interactions. However, they are not strong enough in comparison with the HS−LS energy gap and result in a relatively gradual spin transition for the complex. This example shows that the simple linking of active sites in the polymeric network is not in itself a sufficient condition to generate systems with the cooperative character of a spin transition. The presence of effective intermolecular interactions such as hydrogen bonding and/or π-stacking, favouring the efficient spreading of the intermolecular interactions, as well as the rigidity and conjugated nature of the chemical bridges, can contribute to the cooperativity.

4. Conclusions and Perspectives

To date, one of the most exciting perspectives in molecular science concerns the use of molecules or molecular assemblies as the active elements in devices for signal processing and information storage systems. Spin crossover and, in general, molecular bistability offer prospects for sensitivity and selectivity levels that cannot be reached with conventional solid-state materials. However, many fundamental questions remain to be answered. In particular, we need to study the effect of size reduction on the hysteresis behaviour and analyse the parameters determining the switching process (the origin of energy barriers, the mechanism of structural relaxation on both the molecular and macroscopic scales, etc.). From a chemical point of view, challenges in this field involve the problem of size-reduction and optimisation of the photo/piezo/magneto-excitation efficiency.

Acknowledgments

We deeply thank all our collaborators for their help in the realisation of the results reviewed in this paper, namely M.-L. Boillot, K. Boukheddaden, C. Consejo, P. Demont, L. Dubrovinsky, M. Goiran, J. Haasnoot, T. Kitazawa, J.-F. Létard, J. Linares, J. J. McGarvey, H. Paulsen, J.-A. Real, L. Salmon, K. Tanaka, J.-P. Tuchagues, F. Varret, C. Vieu and A. Zwick.

[1] "Topics in Current Chemistry", *Spin Crossover in Transition Metal Compounds I.-III.* (Eds.: P. Gütlich, H.A. Goodwin), **2004**, vol. 233−235.
[2] [2a] P. Gütlich, A. Hauser, H. Spiering, *Angew. Chem. Int. Ed. Engl.* **1994**, *33*, 2024. [2b] P. Gütlich, *Struct. Bonding (Berlin)* **1981**, *44*, 83. [2c] H. A. Goodwin, *Coord. Chem. Rev.* **1976**, *18*, 293. [2d] E. König, *Struct. Bonding (Berlin)* **1991**, *76*, 51. [2e] O. Kahn, *Molecular magnetism*, VCH, New York, **1993**. [2f] H. Toftlund, *Coord. Chem. Rev.* **1989**, *94*, 67. [2g] J. A. Real, in: *Transition Metals in Supramolecular Chemistry* (Ed.: J. P. Sauvage), Wiley, New York, **1999**, p. 54.
[3] [3a] L. Cambi, A. Cagnasso, *Atti Accad. Naz. Lincei* **1931**, *13*, 809. [3b] L. Cambi, L. Szegö, *Ber. Dtsch. Chem. Ges.* **1931**, *64*, 259.
[4] W. A. Baker, H. M. Bobonich, *Inorg. Chem.* **1964**, *3*, 1184.
[5] E. König, K. Madeja, *J. Chem. Soc., Chem. Commun.* **1966**, 61.
[6] http://iacgu7.chemie.uni-mainz.de/toss/ [Philipp Gütlich (Mainz, Germany), Wolfgang Linert (Wien, Austria), François Varret (Versailles, France), Olivier Kahn (Bordeaux, France), Jaap G. Haasnoot (Leiden, The Netherlands), Jose A. Real (Valencia, Spain), John J. McGarvey (Belfast, UK), Alfred X. Trautwein (Lübeck, Germany), Hans Toftlund (Odense, Danmark), Andreas Hauser (Genève, Switzerland)].
[7] [7a] O. Kahn, C. J. Martinez, *Science* **1998**, *279*, 44. [7b] O. Kahn, J.-P. Launay, *Chemtronics* **1988**, *3*, 140. [7c] O. Kahn, *Curr. Opin. Solid State Mater. Sci.* **1996**, *1*, 547. [7d] O. Kahn, J. Kröber, C. Jay, *Adv. Mater.* **1992**, *11*, 718.
[8] A. Bousseksou, G. Molnár, P. Demont, J. Menegotto, *J. Mater. Chem.* **2003**, *13* 2069.
[9] A. Bousseksou, C. Vieu, J.-F. Letard, P. Demont, J.-P. Tuchagues, L. Malaquin, J. Menegotto, *Molecular Memory with Spin Crossover Complexes*, French Patent filling, no. 01/11328 (31/08/2001), International extension PCT/FR02/02961, August 29, **2002**.
[10] [10a] J. Kröber, E. Codjovi, O. Kahn, F. Groliere, C. Jay, *J. Am. Chem. Soc.* **1993**, *115*, 9810. [10b] J. Krober, J. P. Audiere, R. Claude, E. Codjovi, O. Kahn, J. Haasnoot, F. Groliere, C. Jay, A. Bousseksou, J. Linares, F. Varret, A. Gonthier-Vassal, *Chem. Mater.* **1994**, *6*, 1404.
[11] [11a] A. Bousseksou, N. Negre, M. Goiran, L. Salmon, J. P. Tuchagues, M. L. Boillot, K. Boukhedaden, F. Varret, *Eur. Phys. J. B* **2000**, *13*, 451. [11b] N. Negre, M. Goiran, A. Bousseksou, J. G. Haasnoot, K. Boukheddaden, S. Askenazy, F. Varret, *Synth. Met.* **2000**, *115*, 289. [11c] N. Nègre, C. Consejo, M. Goiran, A. Bousseksou, F. Varret, J.-P. Tuchagues, R. Barbaste,

S. Askénazy, J. G. Haasnot, *Physica B* **2001**, *294/295*, 91. [11d] A. Bousseksou, K. Bokheddaden, M. Goiran, C. Consejo, M. L. Boillot, J. P. Tuchagues, *Phys. Rev. B* **2002**, *65*, 172412. [11e] C. Conséjo, G. Molnár, M. Goiran, A. Bousseksou, *Polyhedron* **2003**, *22*, 2441. [11f] A. Bousseksou, K. Boukheddaden, M. Goiran, J. P. Tuchagues, F. Varret, "Spin Crossover in Transition Metal Compounds III", in *Top. Curr. Chem.* **2004**, *235*, 65. [11g] F. Varret, S. Arun Salunke, K. Boukheddaden, A. Bousseksou, É. Codjovi, C. Enachescu, J. Linares, *C. R. Chim.* **2003**, *6*, 385.

[12] A. Bousseksou, G. Molnar, J. P. Tuchagues, N. Menendez, E. Codjovi, F. Varret, *C. R. Chim.* **2003**, *6*, 329.

[13] [13a] S. Montant, G. Chastanet, S. Létard, S. Marcen, J. F. Létard, E. Freysz, *7th Spin Crossover Family Meeting*, Seeheim, Germany, March 1, **2002**. [13b]H. W. Liu, K. Matsuda, Z. Z. Gu, K. Takahashi, A. L. Cui, R. Nakajima, A. Fujishima, O. Sato, *Phys. Rev. Lett.* **2003**, *90*, 167403.

[14] [14a] H. Spiering, E. Meissner, H. Köppen, E. W. Müller, P. Gütlich, *Chem. Phys.* **1982**, *68*, 65. [14b] N. Willenbacher, H. Spiering, *J. Phys. C: Solid State Phys.* **1988**, *21*, 1423. [14c] H. Spiering, N. Willenbacher, *J. Phys.: Condens. Matter* **1989**, *1*, 10089. [14d] J. Jung, G. Schmitt, L. Wiehl, A. Hauser, K. Knorr, H. Spiering, P. Gütlich, *Z. Phys. B: Condens. Matter* **1996**, *100*, 523.

[15] J. Wajnflasz, R. Pick, *J. Phys.* **1971**, *32*, C1-91.

[16] [16a] A. Bousseksou, J. Nasser, J. Linares, K. Boukheddaden, F. Varret, *J. Phys. I* **1992**, *2*, 1381. [16b] A. Bousseksou, F. Varret, J. Nasser, *J. Phys. I* **1993**, *3*, 1463. [16c] A. Bousseksou, J. Nasser, J. Linares, K. Boukheddaden, F. Varret, *Mol. Crys. Liq. Cryst.* **1993**, *234*, 269. [16d] A. Bousseksou, H. Constant-Machado, F. Varret, *J. Phys. I* **1995**, *5*, 747. [16e] A. Bousseksou, J. Nasser, F. Varret, *J. Magn. Magn. Mater.* **1995**, *140−144*, 1511.

[17] M. Sorai, S. Seki, *J. Phys. Chem. Solids* **1974**, *35*, 555.

[18] [18a] A. Bousseksou, J. J. McGarvey, F. Varret, J. A. Real, J. P. Tuchagues, A. C. Dennis, M. L. Boillot, *Chem. Phys. Lett.* **2000**, *318*, 409. [18b] N. Moliner, L. Salmon, L. Capes, M. C. Munoz, J. F. Létard, A. Bousseksou, J. P. Tuchagues, J. J. McGarvey, A. C. Dennis, M. Castro, R. Burriel, J. A. Real, *J. Phys. Chem. B* **2002**, *106*, 4276. [18c] G. Molnár, V. Niel, A. B. Gaspar, J.-A. Real, A. Zwick, A. Bousseksou, J. J. McGarvey, *J. Phys. Chem. B* **2002**, *106*, 9701. [18d] K. Hosoya, T. Kitazawa, M. Takahashi, M. Takeda, J. F. Meunier, G. Molnar, A. Bousseksou, *Phys. Chem. Chem. Phys.* **2003**, *5*, 1682. [18e] J. P. Tuchagues, A. Bousseksou, G. Molnar, J. J. Mc Garvey, F. Varret, in "Spin Crossover in Transition Metal Compounds III", *Top. Curr. Chem.* **2004**, *235*, 85. [18f] G. Molnar, T. Kitazava, L. Dubrovinsky, J. J. McGarvey, A. Bousseksou, *J. Phys.: Condens. Matter* **2004**, *16*, S1129−S1136. [18g] T. Tayagaki, A. Galet, M. Carmen Muñoz, G. Molnár, A. Zwick, K. Tanaka, J.-A. Real, A. Bousseksou, *J. Phys. Chem. B.*, submitted.

[19] [19a] G. Baranovic, D. Babic, *Spectrochim. Acta A* **2004**, *60*, 1013. [19b] G. Brehm, M. Reiher, S. Schneider, *J. Phys. Chem. A* **2002**, *106*, 12024. [19c] H. Paulsen, A. X. Trautwein, *Top. Curr. Chem.* **2004**, *235*, 197.

[20] [20a] A. Bousseksou, M. Verelst, H. Constant-Machado, G. Lemercier, J.-P. Tuchagues, F. Varret, *Inorg. Chem.* **1996**, *35*, 110. [20b] A. Bousseksou, L. Salmon, F. Varret, J.-P. Tuchagues, *Chem. Phys. Lett.* **1998**, *282*, 209. [20c] N. Moliner, M. Muñoz, S. Létard, L. Salmon, J.-P. Tuchagues, A. Bousseksou, J.-A. Real, *Inorg. Chem.* **2002**, *41*, 6997.

[21] S. Askénazy, C. Fert, J. Marquez, P. Bellan, P. Wallace, F. Herlach, *Rev. Phys. Appl.* **1986**, *21*, 563.

[22] Y. Qi, E. W. Muller, H. Spiering, P. Gütlich, *Chem. Phys. Lett.* **1982**, *93*, 567.

[23] [23a] J. Lejay, A. G. W. Jansen, P. Wyder, *Phys. Rev. B* **1991**, *43*, 8196. [23b] Y. Garcia, O. Kahn, J.-P. Ader, A. Buzdin, Y. Meurdesoif, M. Guillot, *Phys. Lett. A* **2000**, *271*, 145.

[24] [24a] C. P. Slichter, H. G. Drickamer, *J. Chem. Phys.* **1971**, *56*, 2142. [24b] J. R. Ferraro, *Coord. Chem. Rev.* **1979**, *29*, 1. [24c] E. Meissner, H. Köppen, C. P. Kohler, H. Spiering, P. Gütlich, *Hyperfine Interact.* **1986**, *28*, 799. [24d] P. Adler, H. Spiering, P. Gütlich, *J. Phys. Chem. Solids* **1989**, *50*, 587. [24e] V. Ksenofontov, G. Levchenko, H. Spiering, P. Gütlich, J.-F. Létard, Y. Bouhedja, O. Kahn, *Chem. Phys. Lett.* **1998**, *294*, 545. [24f] V. Ksenofontov, H. Spiering, A. Schreiner, G. Levchenko, H. A. Goodwin, P. Gütlich, *J. Phys. Chem. Solids* **1999**, *60*, 393. [24g] S. Schenker, A. Hauser, W. Wang, I. Y. Chan, *Chem. Phys. Lett.* **1998**, *297*, 281. [24h] A. Hauser, H. Romstedt, J. Jeftic, *J. Phys. Chem. Solids* **1996**, *57*, 1743. [24i] J. Jeftic, A. Hauser, *J. Phys. Chem. B* **1997**, *101*, 10262. [24j] E. Codjovi, N. Menéndez, J. Jeftic, F. Varret, *C. R. Acad. Sci., Ser. IIc: Chim.* **2001**, *4*, 181. [24k] V. Ksenofontov, A. B. Gaspar, P. Gütlich, *Top. Curr. Chem.* **2004**, *235*, 23. [24l] T. Granier, B. Gallois, J. Gaultier, J. A. Real, J. Zarembowitch, *Inorg. Chem.* **1993**, *32*, 5305. [24m] J. J. McGarvey, I. Lawthers, K. Heremans, H. Toftlund, *J. Chem. Soc. Chem. Comm.* **1984**, 1575.

[25] [25a] F. Varret, A. Bleuzen, K. Boukheddaden, A. Bousseksou, E. Codjovi, C. Enachescu, A. Goujon, J. Linares, N. Menendez, M. Verdaguer, *Pure Appl. Chem.* **2002**, *74*, 2159. [25b] G. Molnar, V. Niel, J. A. Real, L. Dubrovinsky, A. Bousseksou, J. J. Mc-Garvey, *J. Phys. Chem. B* **2003**, *107*, 3149.

[26] A. Bousseksou, L. Tommasi, G. Lemercier, F. Varret, J.-P. Tuchagues, *Chem. Phys. Lett.* **1995**, *243*, 493.

[27] M. L. Boillot, J. Zarembowitch, J. P. Itié, A. Polian, E. Bourdet, J. Haasnot, *New J. Chem.* **2002**, *26*, 313.

[28] R. Zimmermann, E. König, *J. Phys. Chem. Solids* **1977**, *38*, 779.

[29] J. J. McGarvey, I. Lawthers, *J. Chem. Soc., Chem. Commun.* **1982**, 906.

[30] S. Decurtins, P. Gütlich, C. P. Köhler, H. Spiering, A. Hauser, *Chem. Phys. Lett.* **1984**, *105*, 1.

[31] [31a] A. Hauser, *J. Chem. Phys.* **1991**, *94*, 2741. A. Hauser, *Coord. Chem. Rev.* **1991**, *111*, 275. [31b] A. Hauser, J. Jeftic, H. Romstedt, R. Hinek, H. Spiering, *Coord. Chem. Rev.* **1999**, *190−192*, 491. [31c] A. Hauser, *Top. Curr. Chem.* **2004**, *234*, 155. [31d] F. Varret, K. Boukheddaden, E. Codjovi, C. Enachescu, J. Linarès, *Top. Curr. Chem.* **2004**, *234*, 199.

[32] J.-F. Létard, P. Guionneau, L. Goux-Capes, *Top. Curr. Chem.* **2004**, *235*, 221.

[33] G. S. Matouzenko, A. Bousseksou, S. Lecocq, P. J. van Koningsbruggen, M. Perrin, O. Kahn, A. Collet, *Inorg. Chem.* **1997**, *36*, 2975.

[34] G. S. Matouzenko, A. Bousseksou, S. Lecocq, P. J. van Koningsbruggen, M. Perrin, O. Kahn, A. Collet, *Inorg. Chem.* **1997**, *36*, 5869.

[35] [35a] E. König, K. Madeja, *Inorg. Chem.* **1967**, *6*, 48. [35b] E. König, K. Madeja, K. J. Watson, *J. Am. Chem. Soc.* **1968**, *90*, 1146. [35c] A. Ozarowski, B. R. MacGarvey, A. B. Sarkar, E. Drake, *Inorg. Chem.* **1988**, *27*, 627.

[36] [36a] P. Poganiuch, S. Decurtins, P. Gütlich, *J. Am. Chem. Soc.* **1990**, *112*, 3270. [36b] L. Wiehl, *Acta Crystallogr., Sect. B* **1993**, *49*, 289. [36c] R. Hinek, H. Spiering, D. Schollmeyer, P. Gütlich, A. Hauser, *Chem. Eur. J.* **1996**, *2*, 1427. [36d] G. Matouzenko, G. Vériot, J. P. Dutasta, A. Collet, J. Jordanov, F. Varret, M. Perrin, S. Lecocq, *New J. Chem.* **1995**, *19*, 881. [36e] Y. Garcia, O. Kahn, L. Rabardel, B. Chansou, L. Salmon, J. P. Tuchagues, *Inorg. Chem.* **1999**, *38*, 4663.

[37] G. S. Matouzenko, J.-F. Letard, S. Lecocq, A. Bousseksou, L. Capes, L. Salmon, M. Perrin, O. Kahn, A. Collet, *Eur. J. Inorg. Chem.* **2001**, 2935.

[38] G. S. Matouzenko, A. Bousseksou, S. A. Borshch, M. Perrin, S. Zein, L. Salmon, G. Molnar, S. Lecocq, *Inorg. Chem.* **2004**, *43*, 227.

[39] [39a] M. Mikami, M. Konno, Y. Saito, *Chem. Phys. Lett.* **1979**, *63*, 566. [39b] E. König, G. Ritter, S. K. Kulshreshtha, J. Waigel, L. Sacconi, *Inorg. Chem.* **1984**, *23*, 1241. [39c] C.-C. Wu, J. Jung, P. K. Gantzel, P. Gütlich, D. N. Hendrickson, *Inorg. Chem.* **1997**, *36*, 5339.

[40] [40a] O. Kahn, E. Codjovi, *Philos. Trans. R. Soc. London, Ser. A* **1996**, *354*, 359. [40b] O. Kahn, Y. Garcia, J.-F. Letard, C. Mathonière, *NATO ASI Ser., Ser. C* **1998**, *518*, 127.

[41] [41a] L. G. Lavrenova, V. N. Ikorskii, V. A. Varnek, I. M. Oglez-

neva, S. V. Larionov, *Koord. Khim.* **1986**, *12*, 207. [41b] L. G. Lavrenova, V. N. Ikorskii, V. A. Varnek, I. M. Oglezneva, S. V. Larionov, *Koord. Khim.* **1990**, *16*, 654. [41c] W. Vreugdenhil, J. H. van Diemen, R. A. G. de Graaff, J. G. Haasnoot, J. Reedjik, A. M. van der Kraan, O. Kahn, J. Zarembowitch, *Polyhedron* **1990**, *9*, 2971.

[42] [42a] A. Michalowitch, J. Moscovici, J. Ducourant, D. Cracco, O. Kahn, *Chem. Mater.* **1995**, *7*, 1833. [42b] A. Michalowitch, J. Moscovici, O. Kahn, *J. Phys. IV* **1997**, *7*, C2-633.

[43] [43a] J. A. Real, E. Andrés, M. C. Munoz, M. Julve, T. Granier, A. Bousseksou, F. Varret, *Science* **1995**, *268*, 265. [43b] N. Moliner, C. Munoz, S. Létard, X. Solans, N. Menéndez, A. Goujon, F. Varret, J. A. Real, *Inorg. Chem.* **2000**, *39*, 5390.

[44] G. S. Matouzenko, G. Molnar, N. Bréfuel, M. Perrin, A. Bousseksou, S. A. Borshch, *Chem. Mater.* **2003**, *15*, 550.

Received July 1, 2004

